Dynamic Placement of Plasmonic Hotspots for Super-resolution Surface-Enhanced Raman Scattering

Christopher T. Ertsgaard,[†] Rachel M. McKoskey,[†] Isabel S. Rich,[†] and Nathan C. Lindquist*

Physics Department, Bethel University, St. Paul, Minnesota 55112, United States. [†]These authors contributed equally to this work.

ABSTRACT In this paper, we demonstrate dynamic placement of locally enhanced plasmonic fields using holographic laser illumination of a silver nanohole array. To visualize these focused "hotspots", the silver surface was coated with various biological samples for surface-enhanced Raman spectroscopy (SERS) imaging. Due to the large field enhancements, blinking behavior of the SERS hotspots was observed and processed using a stochastic optical reconstruction microscopy algorithm enabling super-resolution localization of the hotspots to within 10 nm. These hotspots were then shifted across the surface in subwavelength (<100 nm for a wavelength of 660 nm) steps using holographic illumination from a spatial light modulator. This created a dynamic imaging and sensing surface, whereas static illumination would only have produced stationary hotspots. Using this technique, we also show that such subwavelength shifting and localization of plasmonic hotspots has potential for imaging applications. Interestingly, illuminating the surface with randomly shifting SERS hotspots was sufficient to completely fill in a wide field of view for super-resolution chemical imaging.

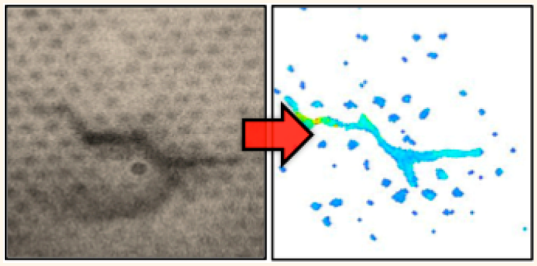

KEYWORDS: plasmonics · nanophotonics · super-resolution microscopy · surface-enhanced Raman scattering · SERS · plasmonic hotspots · computer-generated holography

Diffraction-limited light microscopy cannot achieve the control of optical fields necessary for many demanding applications in nanoscale imaging, sensing, and spectroscopy. To address this, the field of plasmonics[1−3] aims to manipulate light within dimensions much smaller than the optical wavelength by exploiting surface plasmon resonances in metallic nanostructures. Surface plasmons are oscillations of the conduction electrons at the surface of a metal and can squeeze or focus electromagnetic energy into very small volumes. These locally enhanced fields are often called plasmonic "hotspots". Among other emerging applications, plasmons can provide refractive index information for biosensing applications,[4−7] deliver chemical information *via* surface-enhanced Raman spectroscopy (SERS) effects,[8−12] provide superior tip-enhanced imaging resolution,[13] or trap subwavelength objects *via* plasmonic tweezing.[14,15] Plasmonic hotspots have also been used for super-resolution mapping of metallic nanostructures[16−18] and biologically relevant structures.[19] However, to approach the challenges associated with the precise positioning of focused hotspots for sensing, scanning, imaging, or trapping purposes, dynamic placement and characterization of plasmonic hotspots would provide many additional benefits. While focused plasmon waves have been shifted with dynamic illumination of a properly structured surface[20,21] or with shaped ultrafast pulses,[22,23] shifting plasmonic hotspots under full computer control in subwavelength steps, especially for imaging and spectroscopy applications, has not yet been fully explored. Likewise, plasmonic structured illumination microscopy[24−26] and spatially activated plasmonic hotspots[27] have also not been exploited for their super-resolution chemical mapping potential *via* SERS. Beyond chemical "fingerprinting", using SERS for super-resolution imaging has several other advantages over using fluorophore labels, such as the use of longer wavelengths that would inflict less sample damage. In this paper, we present the use of a spatial light modulator (SLM) and computer-controlled holographic laser

* Address correspondence to n-lindquist@bethel.edu.

Received for review August 25, 2014 and accepted September 30, 2014.

Published online September 30, 2014
10.1021/nn504776b

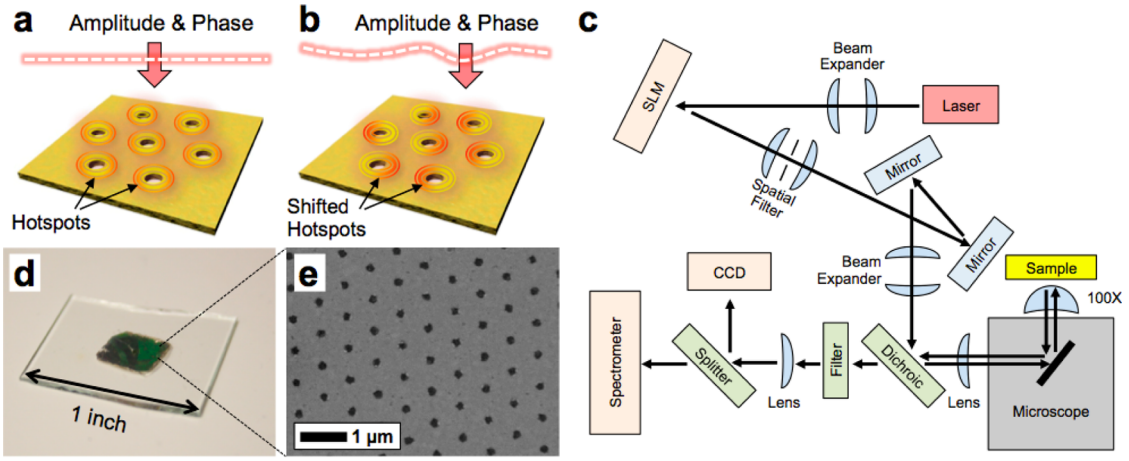

Figure 1. Schematic and nanohole chips. (a) Illuminating an array of plasmonic nanoholes results in a distribution of hotspots. (b) By adjusting the illuminating phase and amplitude, these hotspots can be shifted. (c) Schematic of the microscope system. In conjunction with a spatial filter, the SLM is capable of illuminating a sample with arbitrary amplitude and phase profiles. The reflected light passes through a steep long-pass filter and is sent to a Raman spectrometer and to a CCD camera for wide-field imaging. (d) Photograph of a sample nanohole array chip. (e) Scanning electron micrograph of the nanoholes. The nanoholes have a hexagonal period of 700 nm with a nominal diameter of 150 nm. The 700 nm period of the array allowed strong SERS generation with a 660 nm illumination laser.

illumination to dynamically shift and localize hotspots with sub-diffraction-limited resolution on a silver nanohole array. By properly structuring an illuminating light field with the SLM, we show the possibility of positioning plasmonic hotspots over a metallic nanohole surface on-the-fly. This has potential for high-resolution chemical spectroscopy and imaging. Due to the large field enhancements at the surface, blinking behavior of the SERS hotspots was observed and processed using a custom stochastic optical reconstruction microscopy (STORM) algorithm[28] enabling super-resolution chemical imaging. In our case, using a nanohole array provides tunability, nearest-neighbor coupling for plasmonic control of the hotspots within and around a single nanohole, as well as relatively large SERS signals[10] compared to individual holes.[29] Finally, we show the importance of dynamically shifting these hotspots[27] since static illumination of a plasmonic surface will produce only static plasmonic hotspots. Interestingly, even illuminating the surface with randomly varying phase profiles shifts the hotspots sufficiently to achieve high-resolution SERS imaging of a single strand of collagen protein fibrils. This random illumination technique[30] eliminates the need to solve a difficult inverse problem for specifically tailored hotspot patterns.[20,21]

RESULTS AND DISCUSSION

To generate plasmonic hotspots, a metallic nanoscale surface must be utilized.[31] In this paper, we used a hexagonal array of nanoholes through a 50 nm thick silver film. This nanohole array pattern, once illuminated, will generate plasmons over the surface, causing enhanced transmission effects[32] as well as localized hotspots in and around the nanoholes. Such substrates have been used extensively for surface plasmon resonance biosensing.[6] The localized and enhanced electromagnetic fields also lead to SERS from any proximate molecules.[10] Upon excitation with light, propagating plasmon waves couple each nanohole to its neighbors, giving the ability to manipulate the field profile in and around the nanoholes by illuminating any neighboring nanoholes. In this way, tailoring the illumination amplitude and phase allows us to shift these plasmonic hotspots in and around single nanoholes for dynamic imaging and SERS. Figure 1a,b shows this conceptually. Figure 1c shows a schematic of the microscope illumination system with a 660 nm laser (Laser Quantum) and a phase-only SLM (Hamamatsu). With a proper phase pattern, the SLM is capable of controlling both the amplitude and phase of the illuminating light field. Specifically, by mixing our desired hologram with a grating function, the phase-only SLM can be programmed to diffract any unwanted amplitudes to be blocked by a spatial filter, thus retaining full amplitude and phase control of the illumination.[33]

The silver nanohole arrays were produced *via* a template stripping method.[34] Briefly, a commercially available 700 nm period hexagonal hole patterned silicon template was used, as in our previous work.[35] The template can be reused dozens of times and produces high-quality nanohole arrays over a large area (Figure 1d,e). To coat the nanohole chips with test molecules of interest, the substrates were then submerged in a solution of hexadecanethiol, and imaging was achieved *via* a STORM process of the blinking SERS hotspots. Figure 2a shows a characteristic SERS spectrum from the monolayer of hexadecanethiol, whereas Figure 2b shows the spectrum blinking in time. This blinking behavior, due to its inherently stochastic nature, can be used for super-resolution image processing[19] and SERS hotspot localization.[9] Briefly, using

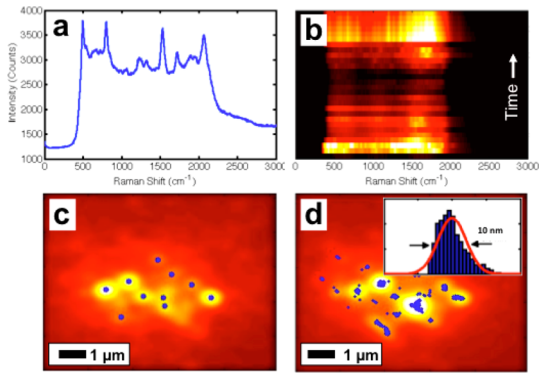

Figure 2. Super-resolution chemical imaging. (a) Experimental SERS spectrum for a hexadecanethiol monolayer on the nanohole substrate. (b) Compilation of 40 hexadecanethiol spectra blinking in time. (c) One frame of the SERS blinking on the nanohole sample illuminated with a wide, slightly defocused laser beam. The blue dots represent the super-resolution hotspot localization for the particular frame. See Supporting Information for further details. (d) Final super-resolution image for all the frames. The image represents an average of all SERS blinking, and the blue dots represent the super-resolution hotspot localization for all frames. (Inset) Single hotspots could be localized to within 10 nm.

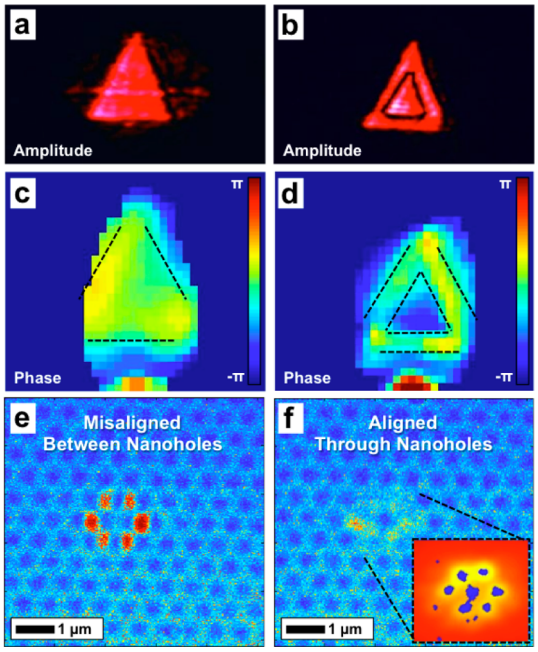

Figure 3. Amplitude and phase control of the illumination profile. (a) Amplitude image of a sample triangle-shaped hologram with a flat phase profile. (b) Amplitude image of the same triangle but with a central triangular patch that is π radians out of phase. (c) Shack–Hartmann phase image of the triangle in (a), verifying the flat phase profile. (d) Phase image of the triangle in (b) verifying the desired π radians phase shift. The scale bar is in radians. Panels (a–d) show complete and arbitrary control of the amplitude and phase of the illumination profile. (e) Images of a hexagonal array of illumination points on the nanohole array. The phase of each of the points is controlled independently. (f) Hexagonal array of illumination points aligned to transmit through the nanoholes. (Inset) In this case, bright SERS hotspots are seen for the surrounding holes as well as from plasmon scattering toward the central nanohole. Panels (e,f) are viewed on the EM-CCD and illuminated with the white light from the microscope (blue tint) as well as the laser (red spots).

the wide-field electron-multiplying (EM) CCD (PCO) and a slightly defocused laser with a 100× (NA = 0.9) objective, SERS blinking was recorded over several frames. Once recorded, the images were transferred to a custom MATLAB script that could detect and localize each SERS hotspot that appeared with a two-dimensional centroid-fitting algorithm. The coordinates of these hotspots, for each frame, could then be mapped (Figure 2c,d) to within 10 nm, creating a single high-resolution image. For further imaging applications, rat-tail collagen was use, as described below. These samples were examined *via* SERS[36] in the same way as the hexadecanethiol samples. More details on the imaging algorithm and data analysis are given in Supporting Information.

In order to dynamically shift the static SERS hotspots shown in Figure 2, customized phase and amplitude illumination profiles were created (Figure 3). For example, to validate our illumination technique and hologram algorithms, Figure 3a shows a triangular pattern demonstrating full amplitude control of the illuminating field. This hologram was then modified to contain a triangular center that was π out of phase (Figure 3b). This phase profile was confirmed using a Shack–Hartmann wavefront sensor (Thorlabs). Where Figure 3c shows a flat phase front for the triangle pattern of Figure 3a, the π phase shift of Figure 3b is seen clearly in Figure 3d. Finally, Figure 3e shows another computer-generated hologram—in this case a hexagonal array of spots—illuminating the hexagonal array of nanoholes. Using the same hologram algorithms as in Figure 3a–d, we could set the phase of each of the individual spots to arbitrary values. This illumination pattern was then precisely aligned to the individual nanoholes using a nanopositioning stage (Mad City Labs) as seen in Figure 3f. In this way, plasmons scattering from each neighboring nanohole toward the central nanohole can be controlled in both amplitude and phase. The hotspot of the central nanohole is thus a product of the scattered plasmons only. Once the hologram was perfectly aligned (Figure 3f), a clear central hotspot was observed (inset). Only the nanoholes that were directly illuminated as well as the central nanohole (which has six nearest neighbors that were illuminated) were detected and localized.

Figure 4 shows the ability to shift the single central hotspot with super-resolution localization and dynamic illumination of the six surrounding nanoholes. Initially, COMSOL simulations were used to determine six phase values for each of the six points (Figure 3e,f) surrounding a central nanohole. While the simulations were in this case trial-and-error, the phase values of {0, 225, 315, 45, 315, 225} degrees (counterclockwise from the right) yielded a shift in the central hotspot position from the left side to the right side of the

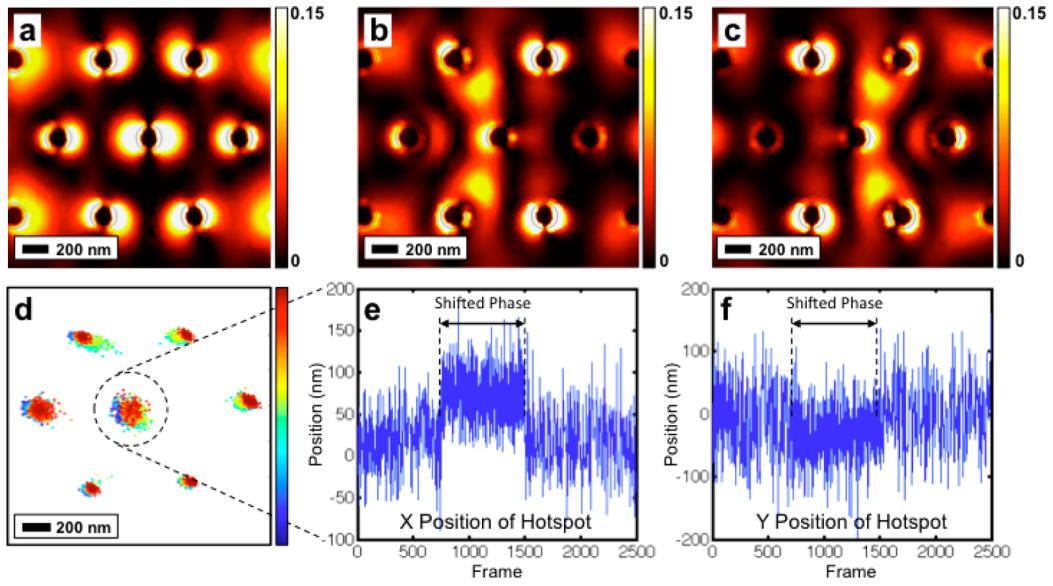

Figure 4. Super-resolution shifting of plasmonic hotspots. (a) COMSOL simulation of a hexagonal array of nanoholes illuminated with a flat phase profile. (b) Adjusting the phase of the six illuminating spots shifts the central hotspot to the left and (c) to the right. (d) Experimental super-resolution image displaying shifts of the central hotspot over the course of 2500 frames. After 750 frames, the phase of the illumination was toggled as explained in the text and toggled back at frame 1500. The coloring scale represents the frame number (blue = frame #1; red = frame #2500). (e) The *x* position of the central hotspot *versus* frame number. The *x* position increased by ~100 nm at frame 750, corresponding to a shift to the right and then dropped back at frame 1500 when the phase was changed to its original state. (f) The *y* position of the central hotspot *versus* frame number. The *y* position shifted downward slightly by ~20 nm.

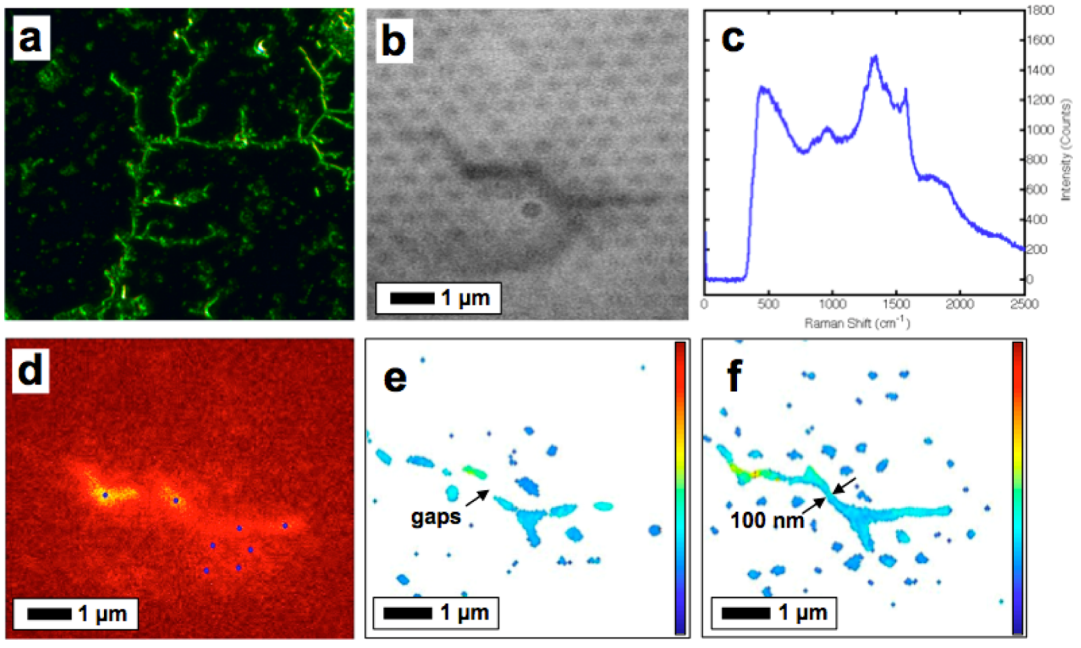

Figure 5. Super-resolution imaging of collagen fibrils. (a) Dark-field optical micrograph of the collagen fibrils on a glass coverslip. (b) Diffraction-limited optical micrograph of a single fibril on the nanohole array substrate. (c) SERS spectrum of a fibril and (d) image of the blinking SERS hotspots. (e) Super-resolution image of 1500 frames taken without shifting the hotspots or phase profile of the illuminating beam. There are obvious gaps in the final image. (f) Image obtained from 1500 total frames after randomly shifting the phase profile of the illuminating beam every 100 frames. The gaps from (e) have been filled in, and the image contains much more detail. Panels (b,d–f) are all of the same area on the sample. The color scale in panels (e,f) represents the relative intensity (arbitrary units) of the localized SERS hotspot.

nanohole (Figure 4a–c). In order to see this shift experimentally, two illumination patterns were created: one held the phase values as indicated in Figure 4b, while the other held phase values as presented in Figure 4c. As before, the blinking of the SERS hotspot was used for super-resolution localization as multiple frames were recorded. In this case, however, the illumination pattern was toggled in real-time.

Figure 4d shows the final recorded image of the six surrounding hotspots including the central hotspot that resulted from the scattered plasmons. The coloring scheme represents the frame number (blue = frame #1; red = frame #2500). The green dots therefore represent when the hologram illumination was toggled to shift the hotspot location to the right. Figure 4e,f shows the *x* and *y* positions of the central hotspot, respectively. When the hologram was toggled at frame 750, the hotspot shifted ~100 nm to the right, consistent with the COMSOL simulations. The hologram was then toggled back at frame 1500, shifting the hotspot to its original location. The plots have been corrected to remove any systematic drift over the course of the several minutes of image acquisition. The use of a nanohole array may complicate data analysis due to coupling between the SERS emission and the plasmonic modes of the surface.[37] While this current work focuses on the ability to dynamically shift the plasmonic hotspots and hence the SERS centroids, efforts are currently underway to examine these coupling effects for our particular structures.

Shifting of the SERS hotspots, as shown in Figure 4, was further applied to test chemical imaging potential. To accomplish this, a larger 10 × 10 hexagonal dot array was rendered, covering more of the hexagonal array. The new hologram was aligned with the nanoholes as in Figure 3f and on top of a ~5 μm long collagen fibril (Figure 5a,b). Each of the hologram's dots was programmed with a random phase value of either 90, 180, 270, or 360°. This created a random placement of the hotspots over the illumination area. Although specific predetermined positioning of the hotspots is possible, as shown earlier, solving for those values would take considerable effort. Instead, a random phase mask still proved sufficient to create the blinking SERS hotspots (Figure 5c) for super-resolution localization (Figure 5d). With a static random phase mask, the randomly placed SERS hotspots remained in place, leaving large gaps in the final rendered image (Figure 5e). By randomly shuffling the phase values every 100 frames with the same total number of frames as before, better imaging was achieved by filling in these gaps. This is shown in Figure 5f. In this case, the collagen fibril is observed to be around 100 nm thick, consistent with previous observations,[36] and smaller than the diffraction-limited resolution of our microscope. While further work is required to completely fill in the image, these results show that even with relative widely spaced nanofeatures (*i.e.*, the 700 nm period hexagonal array), high-resolution image recovery is possible. Finally, more complicated precise positioning of the hotspots may not be necessary[20] since we show that sub-diffraction-limited imaging can be accomplished by combining a SERS/STORM process with illumination by a randomly varying phase mask.

CONCLUSION

We have shown sub-diffraction-limited placement and positioning of plasmonic hotspots that has potential for super-resolution chemical imaging applications. In our case, illuminating individual nanoholes with both amplitude and phase control allowed the shifting of the hotspots within and around the nanoholes. Super-resolution STORM algorithms were used to localize the blinking SERS hotspots to within 10 nm. Our results demonstrated dynamic shifting of single hotspots and may have further application in plasmonic tweezers and nanoparticle manipulation. The results presented in this paper may also have applications in super-resolution chemical imaging or provide insight into the generation and control of plasmonic hotspots. In particular, with careful design of the substrate beyond a relatively simple array of nanoholes, higher resolution and imaging performance can be expected. Finally, our experiments made use of relatively complicated SLM illumination to demonstrate precise hotspot positioning. However, in principle, the imaging results shown would not require such a setup, and a random phase mask could easily be generated in a more cost-effective manner.

METHODS

Nanohole chips were fabricated with a template stripping process. After removing excess silver from any previous depositions, the silicon template (LightSmyth Technologies) was submersed in a H_2O_2/H_2SO_4 (1:1) solution for 10 min. After being washed with deionized water, a 50 nm layer of silver was deposited onto the template using a thermal evaporator (Oxford Vacuum Science) at a rate of 30 nm/min. Finally, a small drop of Norland 61 optical adhesive was applied to the silver and covered with a clean microscope slide. After curing, the patterned silver was stripped from the silicon template, revealing the silver nanohole array. To coat the nanohole chips with test molecules of interest, the nanohole substrates were submerged in a solution of 10 mM hexadecanethiol in ethanol and left for 6 h. After a rinse in ethanol and drying in a stream of compressed air, samples were imaged in the microscope. Rat-tail collagen was obtained from Sigma-Aldrich in powder form. The collagen was mixed to a concentration of 1 mg/mL in 20 mM acetic acid. Assembly was induced by diluting 0.1 mg of the collagen mixture in 1 mL of a phosphate buffered saline solution. Small 1 mL samples were incubated in a 37 °C water bath for 1 h, and then a 0.1 mL aliquot was deposited onto the silver nanohole array. After 30 min, the sample was washed with deionized water and dried with compressed air. COMSOL modeling used a simulation domain large enough to cover a roughly 3 μm × 3 μm × 4 μm volume. The illuminating light was modeled as several focused Gaussian beams on the nanoholes, each with separate amplitude and phase values. Perfectly matched layers were used to minimize boundary reflections, and the mesh was small enough to fully resolve the 50 nm thick and 200 nm diameter nanoholes. SERS imaging was obtained with steep long-pass and dichroic beam splitter filters from

Semrock, an EM-CCD from PCO, and an imaging spectrometer from Horiba. The use of an imaging spectrometer allowed us to extract a full SERS spectrum from a single diffraction-limited spot on the array. Because the SERS image displayed significant blinking behavior, the local spectrum would also vary in time. For more information on the super-resolution imaging algorithms, see Supporting Information.

Conflict of Interest: The authors declare no competing financial interest.

Acknowledgment. This research was supported by an NSF Research in Undergraduate Institutions (RUI) grant (CHE-1306642). Parts of this research were also supported by the Minnesota Space Grant Consortium (MnSGC), part of the NASA funded National Space Grant College and Fellowship Program. Finally, the authors thank B.P. Heppner, C.J. Norman, A.Y. Ash, and C.W. Hoyt for initial SERS tests, and S.N. Elliott for help with thiol chemistry protocols.

Supporting Information Available: More experimental details. This material is available free of charge *via* the Internet at http://pubs.acs.org.

REFERENCES AND NOTES

1. Barnes, W. L.; Dereux, A.; Ebbesen, T. W. Surface Plasmon Subwavelength Optics. *Nature* **2003**, *424*, 824–830.
2. Polman, A. Plasmonics Applied. *Science* **2008**, *322*, 868–869.
3. Ozbay, E. Plasmonics: Merging Photonics and Electronics at Nanoscale Dimensions. *Science* **2006**, *311*, 189–193.
4. Brolo, A. G. Plasmonics for Future Biosensors. *Nat. Photonics* **2012**, *6*, 709–713.
5. Anker, J. N.; Hall, W. P.; Lyandres, O.; Shah, N. C.; Zhao, J.; Van Duyne, R. P. Biosensing with Plasmonic Nanosensors. *Nat. Mater.* **2008**, *7*, 442–453.
6. Gordon, R.; Sinton, D.; Kavanagh, K. L.; Brolo, A. G. A New Generation of Sensors Based on Extraordinary Optical Transmission. *Acc. Chem. Res.* **2008**, *41*, 1049–1057.
7. Lindquist, N. C.; Lesuffleur, A.; Im, H.; Oh, S. H. Sub-micron Resolution Surface Plasmon Resonance Imaging Enabled by Nanohole Arrays with Surrounding Bragg Mirrors for Enhanced Sensitivity and Isolation. *Lab Chip* **2009**, *9*, 382–387.
8. Stiles, P. L.; Dieringer, J. A.; Shah, N. C.; Van Duyne, R. P. Surface-Enhanced Raman Spectroscopy. *Annu. Rev. Anal. Chem.* **2008**, *1*, 601–626.
9. Stranahan, S. M.; Willets, K. A. Others, Super-resolution Optical Imaging of Single-Molecule SERS Hot Spots. *Nano Lett.* **2010**, *10*, 3777–3784.
10. Brolo, A. G.; Arctander, E.; Gordon, R.; Leathem, B.; Kavanagh, K. L. Nanohole-Enhanced Raman Scattering. *Nano Lett.* **2004**, *4*, 2015–2018.
11. Lesuffleur, A.; Kumar, L. K. S.; Brolo, A. G.; Kavanagh, K. L.; Gordon, R. Apex-Enhanced Raman Spectroscopy Using Double-Hole Arrays in a Gold Film. *J. Phys. Chem. C* **2007**, *111*, 2347–2350.
12. Bantz, K. C.; Meyer, A. F.; Wittenberg, N. J.; Im, H.; Kurtulus, Ö.; Lee, S. H.; Lindquist, N. C.; Oh, S. H.; Haynes, C. L. Recent Progress in SERS Biosensing. *Phys. Chem. Chem. Phys.* **2011**, *13*, 11551–11567.
13. Lindquist, N. C.; Jose, J.; Cherukulappurath, S.; Chen, X.; Johnson, T. W.; Oh, S.-H. Tip-Based Plasmonics: Squeezing Light with Metallic Nanoprobes. *Laser Photonics Rev.* **2013**, *7*, 453–477.
14. Juan, M. L.; Righini, M.; Quidant, R. Plasmon Nano-optical Tweezers. *Nat. Photonics* **2011**, *5*, 349–356.
15. Righini, M.; Zelenina, A.; Girard, C.; Quidant, R. Parallel and Selective Trapping in a Patterned Plasmonic Landscape. *Nat. Phys.* **2007**, *3*, 477–480.
16. Weber, M. L.; Willets, K. A. Correlated Super-resolution Optical and Structural Studies of Surface-Enhanced Raman Scattering Hot Spots in Silver Colloid Aggregates. *J. Phys. Chem. Lett.* **2011**, *2*, 1766–1770.
17. Cang, H.; Labno, A.; Lu, C.; Yin, X.; Liu, M.; Gladden, C.; Liu, Y.; Zhang, X. Probing the Electromagnetic Field of a 15-Nanometre Hotspot by Single Molecule Imaging. *Nature* **2011**, *469*, 385–388.
18. Balzarotti, F.; Stefani, F. D. Plasmonics Meets Far-Field Optical Nanoscopy. *ACS Nano* **2012**, *6*, 4580–4584.
19. Ayas, S.; Cinar, G.; Ozkan, A. D.; Soran, Z.; Ekiz, O.; Kocaay, D.; Tomak, A.; Toren, P.; Kaya, Y.; Tunc, I.; *et al.* Label-Free Nanometer-Resolution Imaging of Biological Architectures through Surface Enhanced Raman Scattering. *Sci. Rep.* **2013**, *3*, 2624.
20. Gjonaj, B.; Aulbach, J.; Johnson, P. M.; Mosk, A. P.; Kuipers, L.; Lagendijk, A. Active Spatial Control of Plasmonic Fields. *Nat. Photonics* **2011**, *5*, 360–363.
21. Kao, T.; Rogers, E.; Ou, J.; Zheludev, N. Digitally Addressable Focusing of Light into a Subwavelength Hot Spot. *Nano Lett.* **2012**, *12*, 2728–2731.
22. Aeschlimann, M.; Bauer, M.; Bayer, D.; Brixner, T.; De Abajo, F. J. G.; Pfeiffer, W.; Rohmer, M.; Spindler, C.; Steeb, F. Adaptive Subwavelength Control of Nano-optical Fields. *Nature* **2007**, *446*, 301–304.
23. Aeschlimann, M.; Bauer, M.; Bayer, D.; Brixner, T.; Cunovic, S.; Dimler, F.; Fischer, A.; Pfeiffer, W.; Rohmer, M.; Schneider, C.; *et al.* Spatiotemporal Control of Nanooptical Excitations. *Proc. Natl. Acad. Sci. U.S.A.* **2010**, *107*, 5329–5333.
24. Wei, F.; Liu, Z. Plasmonic Structured Illumination Microscopy. *Nano Lett.* **2010**, *10*, 2531–2536.
25. Ponsetto, J. L.; Wei, F.; Liu, Z. Localized Plasmon Assisted Structured Illumination Microscopy for Wide-Field High-Speed Dispersion-Independent Super Resolution Imaging. *Nanoscale* **2014**, *6*, 5807–5812.
26. Wei, F.; Lu, D.; Shen, H.; Wan, W.; Ponsetto, J. L.; Huang, E.; Liu, Z. Wide Field Super-resolution Surface Imaging through Plasmonic Structured Illumination Microscopy. *Nano Lett.* **2014**, *14*, 4634–4639.
27. Kim, K.; Oh, Y.; Lee, W.; Kim, D. Plasmonics-Based Spatially Activated Light Microscopy for Super-resolution Imaging of Molecular Fluorescence. *Opt. Lett.* **2010**, *35*, 3501–3503.
28. Rust, M. J.; Bates, M.; Zhuang, X. Sub-diffraction-Limit Imaging by Stochastic Optical Reconstruction Microscopy (STORM). *Nat. Methods* **2006**, *3*, 793–796.
29. Wei, H.; Håkanson, U.; Yang, Z.; Höök, F.; Xu, H. Individual Nanometer Hole−Particle Pairs for Surface-Enhanced Raman Scattering. *Small* **2008**, *4*, 1296–1300.
30. Mudry, E.; Belkebir, K.; Girard, J.; Savatier, J.; Moal, E. L.; Nicoletti, C.; Allain, M.; Sentenac, A. Structured Illumination Microscopy Using Unknown Speckle Patterns. *Nat. Photonics* **2012**, *6*, 312–315.
31. Lindquist, N. C.; Nagpal, P.; Mcpeak, K. M.; Norris, D. J.; Oh, S.-H. Engineering Metallic Nanostructures for Plasmonics and Nanophotonics. *Rep. Prog. Phys.* **2012**, *75*, 036501.
32. Ebbesen, T. W.; Lezec, H. J.; Ghaemi, H. F.; Thio, T.; Wolff, P. A. Extraordinary Optical Transmission through Subwavelength Hole Arrays. *Nature* **1998**, *391*, 667–669.
33. Liu, L. Z.; Okeeffe, K.; Lloyd, D. T.; Hooker, S. M. General Analytic Solution for Far-Field Phase and Amplitude Control, with a Phase-Only Spatial Light Modulator. *Opt. Lett.* **2014**, *39*, 2137–2140.
34. Nagpal, P.; Lindquist, N. C.; Oh, S. H.; Norris, D. J. Ultrasmooth Patterned Metals for Plasmonics and Metamaterials. *Science* **2009**, *325*, 594–597.
35. Lindquist, N. C.; Turner, M. A.; Heppner, B. P. Template Fabricated Plasmonic Nanoholes on Analyte-Sensitive Substrates for Real-Time Vapor Sensing. *RSC Adv.* **2014**, *4*, 15115–15121.
36. Gullekson, C.; Lucas, L.; Hewitt, K.; Kreplak, L. Surface Enhanced Raman Spectroscopy of Collagen I Fibrils. *Biophys. J.* **2011**, *100*, 1837–1845.
37. Willets, K. A. Super-resolution Imaging of Interactions between Molecules and Plasmonic Nanostructures. *Phys. Chem. Chem. Phys.* **2013**, *15*, 5345–5354.